



***Título:***

Design of a current harmonic detector method applied in photovoltaic inverters with ancillary service capability

***Autores:***

R. C. de Barros, W. V. Ribeiro, G. L. E. Mata, L. S. Xavier, A. F. Cupertino and H. A. Pereira.

***Publicado em:***

8th International Symposium on Power Electronics for Distributed Generation Systems (PEDG)

***Data da publicação:***

2017

***Citação para a versão publicada:***

R. C. de Barros, W. V. Ribeiro, G. L. E. Mata, L. S. Xavier, A. F. Cupertino and H. A. Pereira, "Design of a current harmonic detector method applied in photovoltaic inverters with ancillary service capability," 2017 IEEE 8th International Symposium on Power Electronics for Distributed Generation Systems (PEDG), Florianopolis, 2017, pp. 1-7.

# Design of a Current Harmonic Detector Method Applied in Photovoltaic Inverters with Ancillary Service Capability

Rodrigo C. de Barros<sup>1</sup>, Wesley V. Ribeiro<sup>1</sup>, Guilherme L. E. Mata<sup>1</sup>, Lucas S. Xavier<sup>1,3</sup>, Allan F. Cupertino<sup>1,2</sup>, Heverton A. Pereira<sup>1</sup>.

<sup>1</sup>Gerência Especialistas em Sistemas Elétricos de Potência  
Universidade Federal de Viçosa  
Av. P. H. Rolfs s/nº, 36570-000  
Viçosa, MG, Brazil  
rodrigocdebarros@gmail.com, v.ribeiro92@hotmail.com,  
glevangelista48@gmail.com, heverton.pereira@ufv.br

<sup>2</sup>Centro Federal de Educação Tecnológica de Minas Gerais  
Av. Amazonas 5253, 30421-169  
Belo Horizonte, Brazil  
allan.cupertino@yahoo.com.br

<sup>3</sup>Graduate Program in Electrical Engineering  
Federal University of Minas Gerais  
Av. Antônio Carlos 6627, 31270-901  
Belo Horizonte, MG, Brazil  
lsantx@gmail.com

**Abstract**— The multifunctional operation of photovoltaic (PV) inverters consists in using the PV inverter for ancillary services as reactive power injection and harmonic current compensation. The multifunctional operation can improve the ac-grid power quality. Thus, this paper presents a dynamic method based on the Second Order Generalized Integrator coupled with a Phase Locked Loop (SOGI-PLL) structure to detect the most predominant harmonic current components in the distribution system. This work intends to show the improvement of the detection method by the use of negative feedback on the SOGI. It is used an extension of this detector to detect multiple harmonic currents according to its amplitude. Besides, the influence of the discretization method is presented and the error in this conversion is analyzed. At last, it can be seen a performance improvement in the detection of the harmonic current amplitudes.

**Keywords**— Solar Power, Harmonic Current Detection, Negative Feedback Method.

## I. INTRODUCTION

The multifunctional operation of photovoltaic (PV) inverters have been strongly studied in the literature. This concept consists in using the PV inverter for ancillary services as reactive power and harmonic current compensation. In this case, the use of multifunctional operation can improve the ac-grid power quality [1], [2].

To improve the grid power quality, the harmonic content in the load current needs to be estimated. After this step, the

inverter can compensate this harmonic current. However, the compensation of all load harmonic current content lead to complex control structures, generally based on multi resonant controllers [1]. In view of this fact, reference [3] proposes a harmonic detection structure, which identifies the greatest harmonic component. Thus, two adaptive resonant controller are employed in this work. The first one to detect the fundamental current, and the second one, the harmonic current.

In literature, some of the commonly harmonic current component detector used are Second Order Generalized Integrators (SOGI) [4], instantaneous power theory [5, 6], conservative power theory [7, 8, 9], Fourier transform [10] and by delayed signal cancellation [11]. However, most of these strategies detect the whole harmonic content from the load, increasing the controller tuning complexity.

Both precision and control complexity are influenced by the controller. Proportional integral (PI) controllers have easier implementation, but present steady state errors due to their limited bandwidth. It can result in a loss of precision. Proportional resonant controllers (PR) present a better precision [12], even though the need of one PR tuned in each frequency being compensated. It can increase control complexity significantly. A solution to obtain a low complexity and precise control is making the controller adaptive to the harmonic current components. Thus, it follows the harmonic variations occurred in the load current [13].

In this work, a harmonic detection is proposed through a cascade association of a SOGI and a synchronous reference frame phase-locked loop (PLL) structure. This method detects the component of higher amplitude [14]. The association of  $n$  structures in series can detect  $n$  harmonic components.

Furthermore, this paper reports a non-detection zone when two harmonics of very close amplitudes are presented in the load current. That detector has a bandpass range, and it is regulated by a SOGI parameter called damping factor. The control of this factor can improve the detection zone until certain distance between the harmonics. However, for two harmonics with very close frequencies it is needed a further method.

In view of the facts aforementioned, this work proposes an improvement in the harmonic detector proposed by [3], reducing the non-detection zone of this structure. This improvement is based on a negative feedback of the estimated harmonic components. When it is used a structure to detect multiple harmonics, the negative feedback method can be very helpful and easily applied. The mathematical modeling of the proposed detector are analyzed to prove the upgrading caused by the negative feedback effect.

In this work, the discretization of the proposed detector is also analyzed. Nowadays, most current controllers are implemented in digital platforms. Hence, the influence of the discretization process should be studied. Thus, the effectiveness of discretization is also evaluated.

This paper contributes to the improvement of the harmonic current detection method proposed. It presents some solution for some problems found in the literature about detection stage, such as the detection of two harmonics of very close frequencies. First, the SOGI structure is presented followed by its transfer function and bode diagram. After, the negative feedback effect is analyzed and, at last, the discretization method is applied, and its error is estimated.

## II. METHODOLOGY

Generally, in single phase PV system, the dc/dc stage with a boost converter is used to keep the desired dc-link voltage constant, as show in Fig.1 (a). The boost control strategy is described in [3].

The inverter control strategy is shown in Fig. 1(b). In the dc-link voltage control, it is used a PI compensator. The compensator calculates the active current amplitude which is injected into the power system. This signal is synchronized

with the PCC voltage, and it is added to the signal from the Harmonic Detector structure.

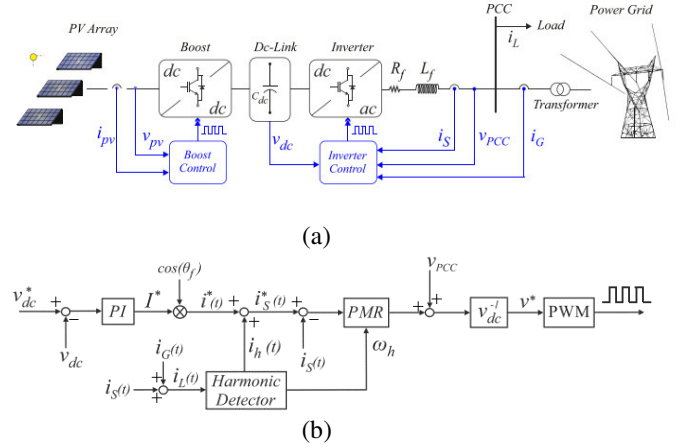


Figure 1. (a) Single-phase grid-connected photovoltaic system. (b) inverter control loop.

### A. Current Harmonic Detector

The current harmonic detector proposed in this work is presented in Fig. 2. The first stage detects the fundamental component of the load current  $i_1(t)$ . The resulting signal consists of the harmonic components. The next stages estimate the harmonic currents according to the largest amplitude. For example, the Stage 2 detects the largest harmonic present in the current; the Stage 3 identify the second largest, and so on, until the last stage (Stage X). A negative feedback of the estimated signals is employed, in order to improve the performance of the harmonic detector. The negative feedback method is the return of part of an output signal to the input, so the output is improved.

Each stage is composed by a SOGI-PLL structure. The Second-Order-Generalized-Integrator (SOGI) is used in [4] for building the Quadrature-Signal-Generator (QSG), and its signal can be used in many applications, such as grid synchronization [5] or for frequency estimation in [6].

The SOGI-PLL structure is illustrated in Fig. 3, and it is applied in the harmonic current extraction, as previously mentioned.

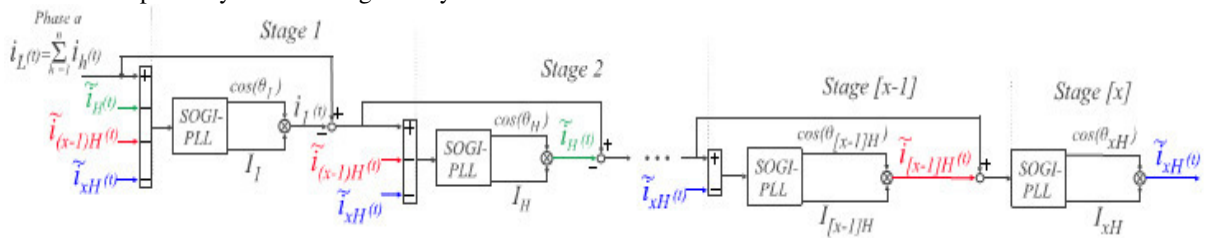


Figure 2. Proposed current harmonic detector.

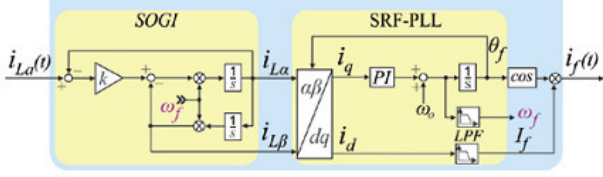


Figure 3. SOGI-PLL Structure.

The transfer function of the SOGI in Fig. 3, is given by:

$$G(s) = \frac{k\omega s}{s^2 + k\omega s + \omega^2} \quad (1)$$

where  $k$  is the damping factor and  $\omega$  is the SOGI operating frequency. The damping factor is responsible for the bandpass range. When  $k$  is increased the bandwidth increases, as seen in [7].

For two harmonics of very close amplitudes, high values of  $k$  can worsen the detection. On the other hand, some low  $k$  values can cause a loss in the detected current amplitude. Plotting the bode diagram of (1) using different values of  $k$ , it can be seen that variation as shown in Fig. 4. Thus, it can be seen a better result for  $k = 0.8$  (tight range and no amplitude loss). After the negative feedback, shown in Fig. 5 (a), the  $k$  value does not have a significant impact in the detection, as can be seen in Fig. 5 (b). The filter does not need to be very tight due to the valley caused by the negative feedback effect. In this work, it is used a  $k = 0.8$ .

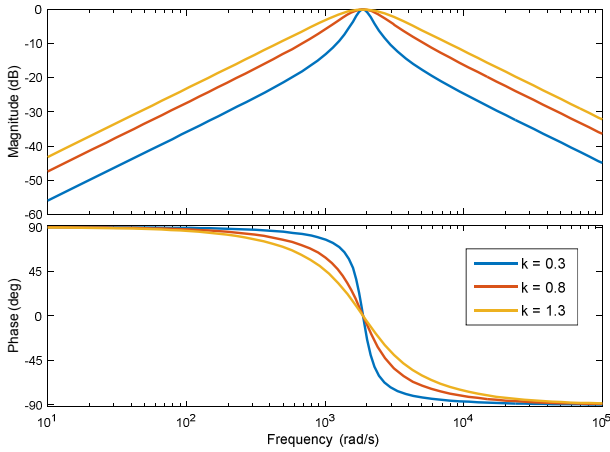


Figure 4. Bode diagram of (1) using different values of  $k$ .

### B. Negative Feedback

The main idea is to apply the negative feedback in order to have better performance during the harmonic detection process. Considering only two stages and disregarding the SRF-PLL dynamics, the block diagram is simplified as shown in Fig. 5(a).  $G_1$  is the SOGI transfer function for the fundamental component detector and  $G_H$  is the SOGI transfer function for the harmonic component.

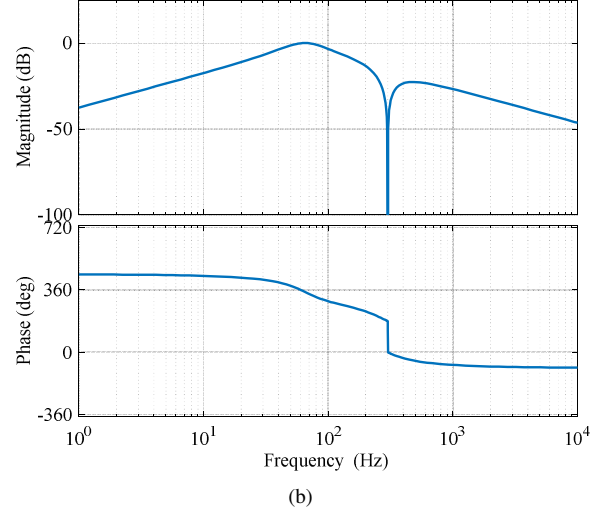
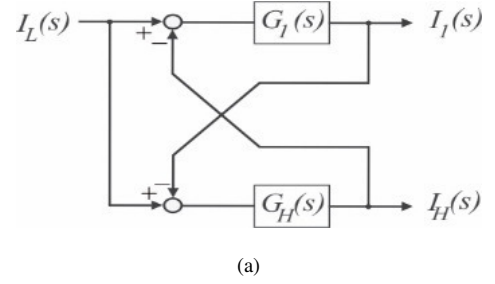


Figure 5. Analysis of the proposed harmonic detector: (a) Simplified structure; (b) bode diagram.

Using the block diagram of Fig. 5 (a), the following transfer functions are obtained:

$$\frac{I_1(s)}{I_L(s)} = \frac{G_1(s) - G_1(s) \times G_h(s)}{1 - G_1(s) \times G_h(s)}, \quad (2)$$

$$\frac{I_H(s)}{I_L(s)} = \frac{G_h(s) - G_1(s) \times G_h(s)}{1 - G_1(s) \times G_h(s)}, \quad (3)$$

which represents the frequency behavior of the proposed harmonic detector. The bode diagram of this transfer function is presented in Fig. 5 (b). In this example, it was considered  $k=0.8$ , and 5th harmonic detection. As observed, the negative feedback introduces an anti-resonance frequency, which attenuates the frequencies different from the detected. Similar results can be obtained when the harmonic estimation is analyzed.

The system described in this work was simulated on the PLECS and Matlab environment. In the single phase case study, the PV array was composed of 2 strings with 10 panels of 250 W connected in series, resulting in a system of 5 kW. The system is represented by the Figure 5. The PV panel utilized in this work has the characteristics presented in Table I.

TABLE I. PV PANEL SPECIFICATION

Parameters	Value
Nominal Power	250W
Short Circuit Nominal Current	$I_{scn} = 8.5 A$
Open Circuit Nominal Voltage	$V_{ocn} = 35.5 V$
Maximum Power Point Current	$I_{mp} = 7.99 A$
Maximum Power Point Voltage	$V_{mp} = 31.29 V$

The system parameters are presented in Table II and the control gain in Table III. The solar irradiance is maintained in 1000 W/m<sup>2</sup>. In the case study, there are two stages. The first SOGI detects the fundamental component of the current and the Second SOGI detects the harmonic presents in the current that flows to the grid.

TABLE II. SIMULATION PARAMETERS

Description	Value
Switching frequency	12 kHz
Sampling frequency	12 kHz
LCL filter inductors	1 mH / 19mΩ
LCL filter capacitor	3.8 μf
LCL filter damping resistance	4 Ω
PCC voltage	220 $V_{rms}$
Dc-link voltage	390 V
Dc-link capacitance	500 μF

TABLE III. CONTROL PARAMETERS OF THE INVERTER

Controllers Gains	Value
dc-link controller	$K_{p\_sdc} = 0.145$ $K_{i\_sdc} = 1.244$
Dc/dc boot converter controllers	$K_{p\_VM} = 1.508$ $K_{i\_VM} = 158.733$ $K_{p\_IM} = 0.193$ $K_{i\_IM} = 0.387$
Resonant Controller	$K_{p\_res} = 14.833$ $K_{i\_res} = 2000$

### III. DISCRETIZATION METHODS

Most current controllers are implemented in digital platforms. Thus, the influence of the discretization process should not be ignored [8]. There are several discrete-time implementations of these controllers. According to [8], because of the narrow band of the harmonic current detector, they present some sensitive to the discretization process. Thus, it is very important to evaluate the effectiveness of the discretization alternatives, providing an accurate resonant frequency. Table I shows some discretization methods.

TABLE IV. RELATIONS FOR DISCRETIZING BY DIFFERENT METHODS

Discretization method	Equivalence
Forward Euler	$s = \frac{1 - z^{-1}}{z^{-1}T_s}$
Backward Euler	$s = \frac{1 - z^{-1}}{T_s}$
Tustin	$s = \frac{2}{T_s} \frac{1 - z^{-1}}{1 + z^{-1}}$

In order to choose the discretization method for the SOGI structure, a study about the frequency error is made in this work, as can be seen in Fig 6. The sampling frequency ( $f_s$ ) is changed from 8 kHz to 18 kHz and component harmonic ( $f_h$ ) is changed from the 2<sup>th</sup> to the 12<sup>th</sup>. As can be observed, the discretization error for the Forward-Backward method results in a large frequency error for low sampling frequencies and for high harmonic components orders comparing to the Tustin-Tustin discretization method. Therefore, in this paper the Tustin-Tustin method is employed in the SOGI structure discretization process.

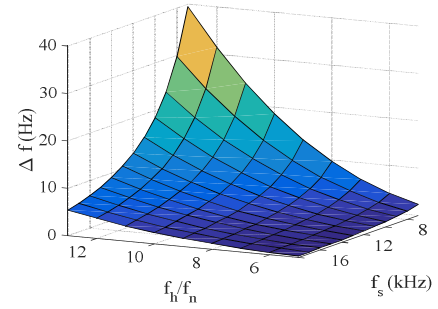


Figure 6. Discretization error as function of sampling frequency and harmonic order: FB discretization method.

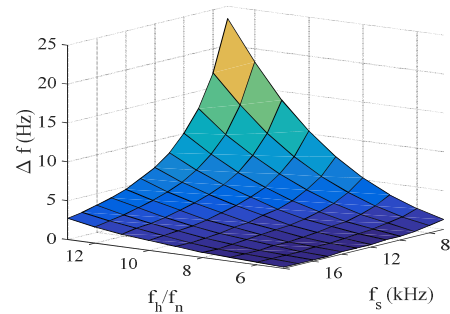


Figure 7. Discretization error as function of sampling frequency and harmonic order: Tustin discretization method.

### IV. CASE STUDY

The nonlinear load is used to simulate the injection of the harmonics components into the grid. The nonlinear load is composed by two different stages. In the first stage there are an injection of the 5<sup>th</sup> harmonic component with 5A and the 7<sup>th</sup> with 2 A. In the second stage, the injection of the fifth

harmonic component is stopped and the 2<sup>th</sup> harmonic injection, with 5 A, is started. In addition, in both stages the fundamental component is injected with 10 A of amplitude. The parameters of the SOGI structure are shown in Table II.

TABLE V. HARMONIC DETECTOR PARAMETERS

Structure	Value
SOGI-PLL Parameters of the 1 <sup>st</sup> Stage	$k = 0.8$ $W_n = 60.2\pi \text{ rad}$
SOGI-PLL Parameters of the 2 <sup>nd</sup> Stage	$k = 0.8$ $W_h = 60.2\pi \cdot 5 \text{ rad (for } t < 3s)$ $W_h = 60.2\pi \cdot 2 \text{ rad (for } t > 3s)$

The first SOGI structure detects the fundamental component of the load current and the second SOGI structure detects the harmonic component with higher amplitude. In particular to this case study, the sampling frequency is 12 kHz and the simulation time is 5 seconds. Also, the Tustin-Tustin discretization method was used on the SOGIs structure.

Also, in this case study, the same simulation is made using the sampling frequency equal to 6 kHz and 12 kHz. The Tustin-Tustin and Forward-Backward discretization method is analyzed when the  $f_s$  is decreased.

In the last part of this work, the negative feedback strategy is applied in a photovoltaic inverter shown in Fig.1 (a). All the parameters used in this simulation are presented in TABLE I, II and III. Also, the nonlinear load is composed by two stages. The first one has an injection of 3<sup>th</sup> harmonic component ha with 5 amperes of amplitude and the 7<sup>th</sup> component harmonic with 1 ampere of amplitude. In the second stage the injection of the 3<sup>th</sup> component is stopped and the 5<sup>th</sup> harmonic component is injected. Therefore the result of the harmonic compensation using negative feedback is analyzed. In addition, the Tustin-Tustin discretization method is used in this simulation.

## V. SIMULATION RESULTS

The harmonic current detection starts at 1.0 seconds of simulation. The injection of the 5<sup>th</sup> harmonic components is kept until the simulation time of 3 seconds and then it is changed to 2<sup>th</sup> harmonic component. During the entire simulation, the 7<sup>th</sup> harmonic component is also injected by the nonlinear load. The current from the nonlinear load and the harmonic spectrum are shown in Fig.7.

The focus of this simulation is to compare the performance of the harmonic detection using negative feedback and the method that already exist, without negative feedback. The results of the amplitude and frequency detection of the harmonics components for both methods are shown in Fig.9 and Fig 10 respectively.

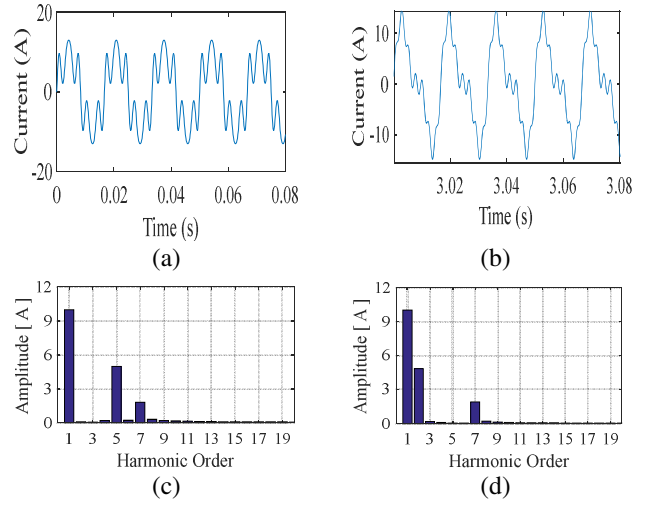


Figure 8. Current load representation: (a) and (c) represent the first stage of the current load and the harmonic spectrum respectively; (b) and (d) represent the second stage of the current load and the harmonic spectrum respectively.

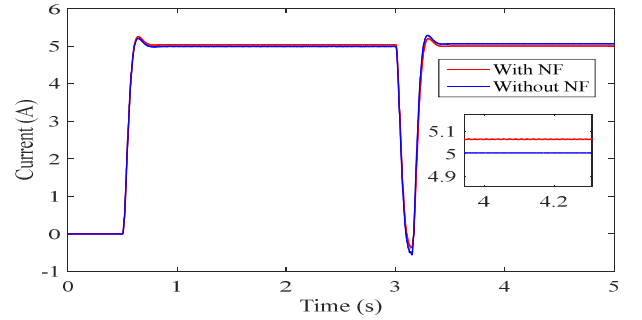


Figure 9. Amplitude harmonic detection using Negative Feedback and without using Negative feedback.

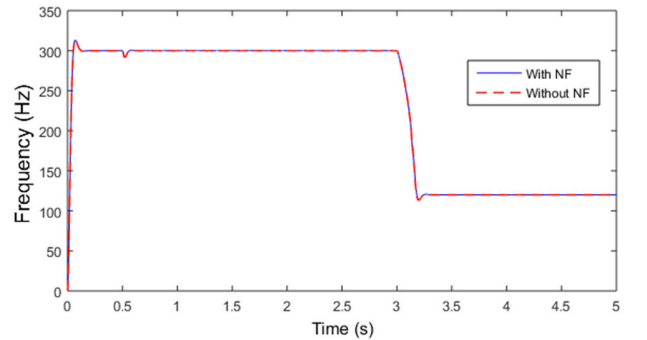


Figure 10. Frequency harmonic detection using Negative Feedback and without using Negative feedback.

As can be seen, both methods detect the harmonic current with the higher amplitude. However, the system using negative feedback detects the harmonic with amplitude closer to 5 A, which is injected to the grid. Also, the results are even improved to the harmonic with high frequency (5<sup>th</sup>). The steady-state error without negative feedback strategy is 1.26% while the steady-state error using negative

feedback is 0.08%. Therefore, the method using negative feedback has improved the harmonic component detection.

In order to check the effect of the sampling frequency in the discretization process of the SOGI structure, the  $f_s$  is changed from 6 kHz to 12 kHz and the amplitude error of the harmonic component are shown in Fig. 11 and Fig. 12, respectively.

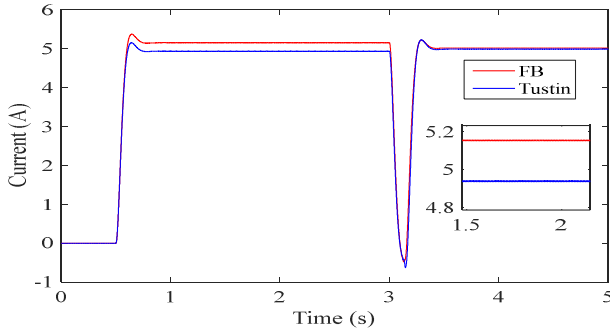


Figure 11. Backward & Forward and Tustin discretization methods with  $f_s$  equal to 6 kHz.

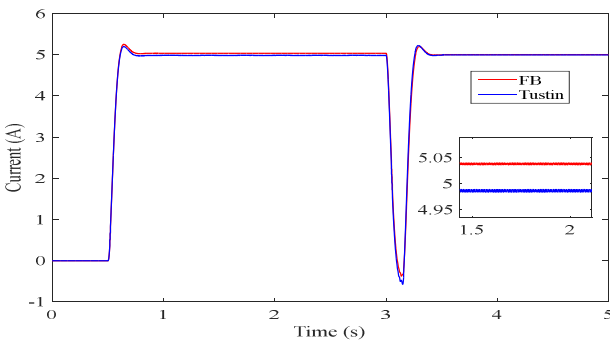


Figure 12. Backward & Forward and Tustin discretization methods with  $f_s$  equal to 12 kHz.

The steady-state error for Forward and Backward using the frequency equal to 6 kHz is around 9.8% and for sampling frequency equal to 12 kHz the steady-state error is around 0.76 %. In the same way, the steady-state error using Tustin-Tustin discretization method for sampling frequency equal to 6 kHz is 1.26 % and for  $f_s$  equal to 12 kHz the steady error is 0.28%. Therefore, it is clear to check the increasing of the steady-state error when the sampling frequency is decreased.

Finally, the negative feedback strategy is applied in an inverter photovoltaic system in order to detect the components harmonics applied to the grid and compensate them.. The load current, the inverter current and the grid current, are shown in Fig.11.

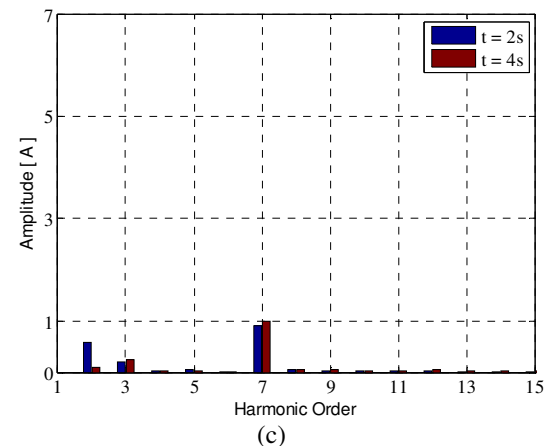
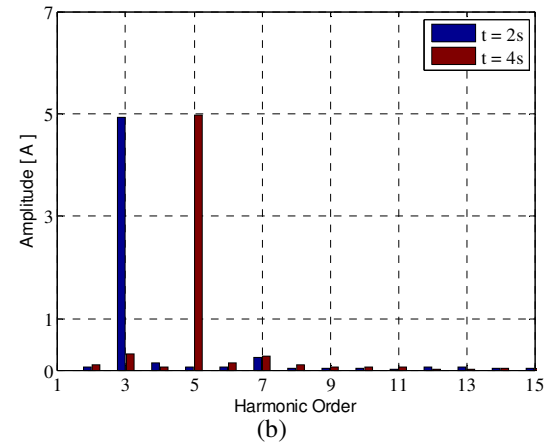
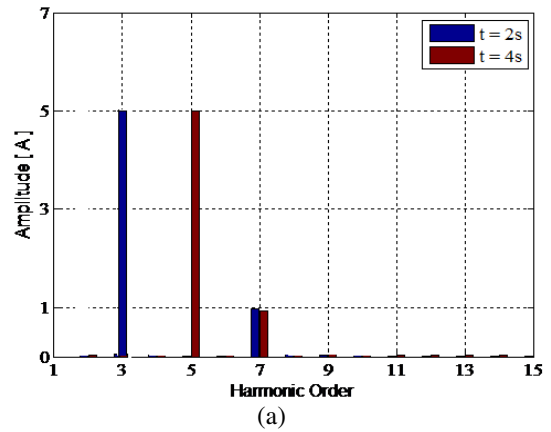


Figure 13. Current harmonic spectrum from the inverter photovoltaic system: (a) Load Current; (b) Inverter Current; (c) Grid Current.

As can be seen, the negative feedback strategy has a considerable performance in a harmonic detection used for harmonic compensation in photovoltaic inverters. The current that flows into the grid has very low amplitude of the harmonics injected in stage1 end 2.

## VI. CONCLUSIONS

This work compares the negative feedback harmonic detector with the method already existent in the literature. As highlighted, the negative feedback method improves the harmonic detection.

Also, two different discretization methods were used in order to analyse the discretization process of the SOGI transfer function. The Tustin-Tustin method is more efficient in the harmonic current amplitude detection. This method presents less error for different frequency harmonic and sampling frequency.

## ACKNOWLEDGMENT

The authors would like to thank to CNPQ, FAPEMIG and CAPES for their assistance and financial support.

## REFERENCES

- [1] J. He, Y. W. Li, F. Blaabjerg and X. Wang, "Active Harmonic Filtering Using Current Controlled Grid-Connected DG Units with Closed-Loop Power Control," *IEEE Transactions on Power Electronics*, vol. 29, pp. 642 – 653, Feb. 2011.
- [2] S. Ozdemir, S. Bayhan, I. Sefa e N. Altin, "Three-phase multilevel grid interactive inverter for PV systems with reactive power support capability," *in Proc. of 2015 First Workshop on Smart Grid and Renewable Energy*, 2015, pp. 1-6
- [3] L. S. Xavier, A. F. Cupertino, J. T. Resende, V. F. Mendes and H. A. Pereira, "Adaptive current control strategy for harmonic compensation in single-phase solar inverters". *Electric Power Systems Research (Print)*, vol. 142, p. 84-95, Jan 2017.
- [4] P. Rodriguez, A. Luna, I. Candela, R. Mujal, R. Teodorescu, F. Blaabjerg, Multiresonant Frequency-Locked Loop for Grid Synchronization of Power Converters Under Distorted Grid Conditions, *Industrial Electronics, IEEE Transactions on* 58 (2011) 127–138.
- [5] H. Akagi, Y. Kanazawa, A. Nabae, Instantaneous Reactive Power Compensators Comprising Switching Devices without Energy Storage Components, *IEEE Trans. Ind. Appl. IA-20* (1984) 625–630.
- [6] E. H. Watanabe, M. Aredes, Active and Reactive Instantaneous Power Theory and Applications - Active Filters and FACTS, *Brazilian Congress of Automatic - CBA* (1998) 81–122
- [7] D. I. Brandão, F. P. Marafão, H. K. M. Paredes, A. Costabeber, Invertercontrol strategy for DG systems based on the Conservative power theory, *in: IEEE Energy Conversion Congress and Exposition*, 2013, pp. 3283–3290. doi:10.1109/ECCE.2013.6647131
- [8] L. S. Xavier, A. F. Cupertino, H. A. Pereira, Adaptive saturation scheme for a multifunctional single-phase photovoltaic inverter, *in: IEEE/IAS International Conference on Industry Applications*, 2014, pp. 1–8
- [9] J. P. Bonaldo, H. K. M. Paredes, J. A. Pomilio, Control of Single-Phase Power Converters Connected to Low Voltage Distorted Power Systems with Variable Compensation Objectives, *IEEE Transactions on Power Electronics* 31 (2016) 2039–2052.
- [10] B. P. McGrath, D. G. Holmes, J. J. H. Galloway, Power converter line synchronization using a discrete Fourier transform (DFT) based on a variable sample rate, *IEEE Transactions on Power Electronics* 20 (2005) 877–884.
- [11] Y. F. Wang, Y. W. Li, Three-Phase Cascaded Delayed Signal Cancellation PLL for Fast Selective Harmonic Detection, *IEEE Transactions on Industrial Electronics* 60 (2013) 1452–1463
- [12] W. Yanfeng, S. Rongyan, G. Xinhua, L. Yan, Y. Hua, The comparative analysis of PI controller with PR controller for the single-phase 4-quadrantrectifier, *in: IEEE Conference and Expo Transportation ElectrificationAsia-Pacific*, 2014, pp. 1–5. doi:10.1109/ITEC-AP.2014.6941089.
- [13] L. S. Xavier, A. F. Cupertino, V. F. Mendes, H. A. Pereira, A novel adaptive current harmonic control strategy applied in multifunctional single phase solar inverters, *in: 13th Brazilian Power Electronics Conference and 1st Southern Power Electronics Conference*, 2015.
- [14] M. Ciobotaru, R. Teodorescu, F. Blaabjerg, A New Single-Phase PLL Structure Based on Second Order Generalized Integrator, *in: IEEE Power Electronics Specialists Conference*, 2006.
- [15] M. Ciobotaru, R. Teodorescu, and F. Blaabjerg, "A new single-phase PLL structure based on second order generalized integrator," *in Proc. 32nd IEEE PESC'06*, Jun. 2006, pp. 1–6.
- [16] P. Rodriguez, A. Luna, M. Ciobotaru, R. Teodorescu, and F. Blaabjerg, "Advanced grid synchronization system for power converters under unbalanced and distorted operating conditions," *in Proc. 32nd IEEE IECON*, Paris, France, Nov. 6–10, 2006, pp. 5173–5178.
- [17] P. Rodriguez, R. Teodorescu, I. Candela, A.V. Timbus, M. Liserre, and F. Blaabjerg, "New Positive-sequence Voltage Detector for Grid Synchronization of Power Converters under Faulty Grid Conditions," *in Proc. IEEE Power Electron. Spec. Conf. (PESC'06)*, Jun. 2006, pp. 1-7.
- [18] Yepes, Alejandro Gómez. Digital resonant current controllers for voltage source converters. *Diss. University of Vigo*, 2011.
- [19] Xin, Zhen, et al. "An improved second-Order generalized integrator based quadrature signal generator." *IEEE Transactions on Power Electronics* 31.1